COVER SHEET

Title: Hyper-Velocity Impact Performance of Foldcore Sandwich Composites

Authors: Nathan Hoch
Chase Mortensen
Juhyeong Lee
Khari Harrison
Kalyan Raj Kota
Thomas Lacy

Paper Number: 97

ABSTRACT

A foldcore is a novel core made from a flat sheet of any material folded into a desired pattern. A foldcore sandwich composite (FSC) provides highly tailorable structural performance over conventional sandwich composites made with honeycomb or synthetic polymer foam cores. Foldcore design can be optimized to accommodate complex shapes and unit cell geometries suitable for protective shielding structures

This work aims to characterize hypervelocity impact (> 2000 m/s, HVI) response and corresponding damage morphologies of carbon fiber reinforced polymer (CFRP) FSCs. A series of normal (0° impact angle) and oblique (45° impact angle) HVI (~3km/s nominal projectile velocity) impact tests were performed on CFRP FSC targets to understand the effects of projectile impact on redirected debris formation, and variable debris cloud expansion. HVI damage in FSC targets were assessed using visual inspection and high-speed imaging analysis. The results from the present study indicate that debris cloud propagation and expansion are strongly influenced by foldcore impact location/angle and open-channel direction. This work serves as a baseline study to understand HVI response of FSC targets and to identify critical FSC design parameters to optimize HVI mitigation performance.

Nathan Hoch, Chase Mortensen, and Juhyeong Lee, Department of Mechanical and Aerospace Engineering, Utah State University, Logan, UT 84322.
Khari Harrison and Thomas Lacy, J. Mike Walker '66 Department of Mechanical Engineering, Texas A&M University, College Station, TX 77843.
Kalyan Raj Kota, George H.W. Bush Combat Development Complex, The Texas A&M University System, College Station, TX, 77807.

INTRODUCTION

Conventional protective structures used in aerospace and military applications are sandwich panels consisting of thin, stiff skins (facing or face-sheet) and a thick, but lightweight core, *i.e.*, honeycomb or synthetic polymer foam. The sandwich panel provides higher bending stiffness with a minimal weight gain. However, due to their closed-cells and sealing structures, sandwich panels with honeycomb and foam cores have limited geometric customization and material selection and are susceptible to water/moisture contamination. An alternative to the legacy sandwich composites with honeycomb/foam core materials is the foldcore sandwich composite (FSC, cf. Fig. 1a)

A foldcore (Fig. 1b) is a core made from a flat sheet of any material that has been folded into a desired pattern. Foldcores can be made of carbon fiber reinforced plastics (CFRP), aluminum, aramids, papers, and plastics [1-7]. The foldcore concept emerged in the 1970s [1] as a possible alternative to legacy cores. The most common folding pattern is the Miura fold named after its inventor Dr. Koryo Miura [8]. In 1972, Dr. Miura concluded that foldcores can be manufactured to have shear modulus comparable to conventional honeycomb core and can be used for free-form structures, high temperature applications, and shock absorption structures. In addition to the benefits outlined by Miura, foldcores have been researched because of their open cell nature. Honeycomb and foam cores have closed-cells and are susceptible to moisture ingress in the presence of cracks on the face-sheet and at the face-sheet/core interfaces. Considerable moisture ingress occurs in honeycomb core sandwich panels used in aircraft control surfaces, landing gear doors and rotor blades [9]. This moisture can cause delamination and debonding failure of sandwich structures. Special equipment (*i.e.*, thermography, ultrasound, neutron radiography) is required to nondestructively detect the presence of moisture [9]. The open cell nature of FSCs (Fig. 1a) allows for moisture evacuation to protect the core from property degradation and parasitic weight.

Figure 1. a) Foldcore sandwich composite (FSC) and b) foldcore.

Many studies [1-4] have characterized quasi-static compression and impact performance of FSCs. Miura-based FSC response to low velocity impact (~10 m/s, LVI) is strongly independent of impact location [1]. Miura FSCs absorb all kinetic energy in high velocity impact (< 2 km/s, HiVI) tests, but with significant back face debonding. The standard Miura foldcore pattern has been modified to improve performance. Researchers have studied curved-crease, indented, cube-strip, and diamond-strip foldcores (Fig. 2) in quasi-static compression and LVI [2-4]. Curved-crease foldcores have demonstrated better LVI energy absorption capability than

straight crease foldcores [2]. Indented-foldcores have shown a more uniform energy absorption under quasi-static compression compared to Miura foldcores [3]. Cube-strip foldcores absorbed more energy than Miura foldcores in quasi-static compression [4].

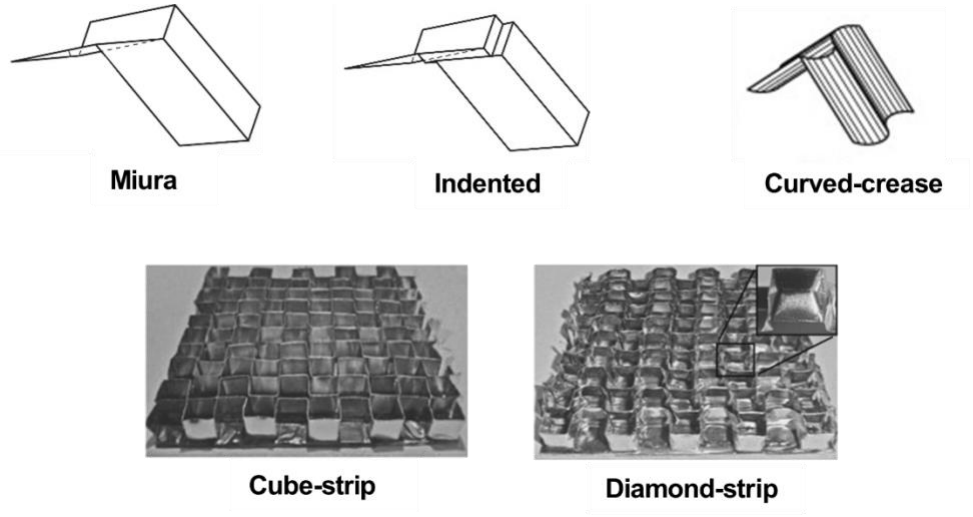

Figure 2. Various foldcore patterns [2-4]

While FSC responses to quasi-static compression, LVI, and HiVI have been previously studied [1-6], their response to hypervelocity impact (> 2 km/s, HVI) is yet unknown. However, the HVI response of legacy core materials has been studied intensively. Honeycomb core sandwich panels were found to perform worse than open-cell foam and Whipple shields in HVI tests performed by NASA [10]. The majority of a honeycomb's cross-section is made of hexagonal pockets of air. Once a projectile has passed through the first face-sheet, it will go through either air or the thin cell wall depending on impact location. FSC cores provide a continuous additional layer of high strength material for impact resistance. It is hypothesized that the continuous material, angled faces, and open channels of foldcore will facilitate redirection of projectiles and debris.

This work aims to characterize the structural response and corresponding damage morphologies of FSCs subjected to HVI. A series of normal (0° impact angle) and oblique (45° impact angle) HVI (~3km/s nominal projectile velocity) impact tests were performed on CFRP FSC targets. Visual inspection and high-speed imaging analysis were used to assess the evolution and shape of debris cloud and associated damage morphology of the FSC targets. Another baseline study is presented in a companion paper titled "Effects of Layup and Impact Orientation on Hypervelocity Impact Response of Carbon Fiber Reinforced Polymer Composites" demonstrating the HVI responses of flat CFRP composite targets impacted at normal and oblique impact angles (0° or 45°).

TECHNICAL BACKGROUND

In the present study, Miura folding-based foldcores and FSCs were fabricated. The Miura core unit cell consists of four angled parallelograms (Fig. 3). The core

geometric parameters include the core height *H*, the cell length *L*, the fold length *I*, the fold angle *α*, the material thickness *t*, and the bend radius *r*. Foldcore mechanical properties are strong functions of these geometric parameters. For instance, an increase in *H*, *I*, *α*, and *t* improve core stiffness and maximum failure load, while a decrease in *L* results in an increase in both stiffness and maximum quasi-static compression failure load [11]. The foldcore geometry and dimensions selected in this study were motivated by those from [12]. TABLE I lists all foldcore geometric parameters measured from actual FSC targets. Note that the bend radius *r* in the table is defined to avoid potential demolding issues and stress concentrations at the contact areas.

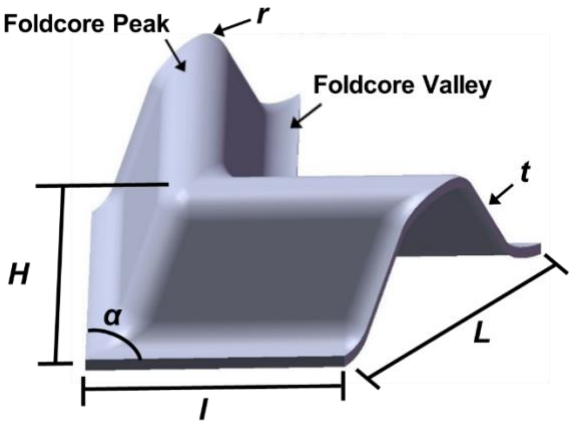

Figure 3. Foldcore unit cell parameters.

TABLE I. FOLDCORE DIMENSIONS

H **(mm)**	***L*** **(mm)**	***I*** **(mm)**	**α (°)**	***t*** **(mm)**	***r*** **(mm)**
16	33	29	87	1.5	4

FSC MANUFACTURING

The foldcores used for HVI tests were manufactured with a discontinuous (or batch) folding process. Discontinuous manufacturing processes are common among researchers when making foldcore test coupons [5, 6]. The up-front material and time costs for discontinuous folding processes are much cheaper than up-front continuous folding processes costs, but the size and number of foldcore samples are limited [7].

The foldcore and each face-sheet were prepared with eight unidirectional ($[0]_8$) CFRP woven fabric prepregs (Hexcel AGP 193-P, 3k AS4/3501-6 carbon/epoxy) [13, 14]. In an early stage of the work, several manufacturing techniques (*i.e.*, compression molding, resin transfer molding, and resin infusion) were applied to fabricate the foldcores. Compression molding was determined as the best foldcore fabrication method for repeatability and consistency in quality. Fig. 4 provides an overview of the foldcore and FSC manufacturing process. In the current study, foldcores were fabricated with an aluminum 6061 two-piece mold. Eight plies of the CFRP prepreg were hand-formed onto the bottom mold piece. This pre-folding process facilitates uniform molding and avoids stretching of the woven fabric prepregs. A perforated release film was placed between the pre-folded laminate and

the top and bottom mold. The entire mold was vacuum bagged and cured according to the manufacturer's recommendation (121°C for 1 hr. followed by 2 hrs. at 177°C) [14]. One hour into the cure cycle, the mold set was momentarily removed from the oven. Note that, at this point in the cure cycle, the resin is in a partially cured stage, and thus the laminate is still malleable. The mold set was then compressed using a 25-ton hydraulic press. Compressing the laminate, while the prepreg is not fully cured, allows conformity to the mold without stretching of the laminates. The compressed mold set was then clamped together and returned to the oven to finish curing. Bonding of foldcore to face-sheets was done with 3M DP420 two-part epoxy. The contact surfaces of the foldcore and face-sheets were abraded prior to bonding to improve their adhesion.

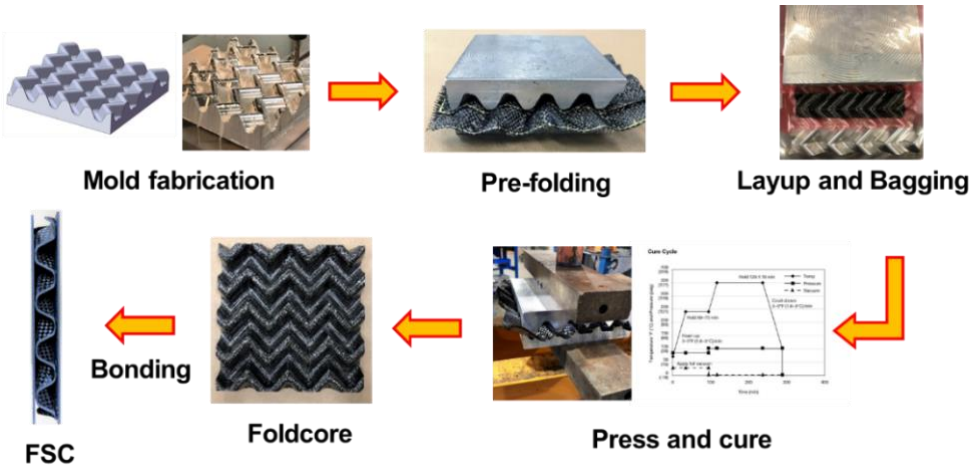

Figure 4. FSC manufacturing process.

After curing, the foldcore and face-sheet had the nominal dimensions of $14 \times 14 \times 1.6$ cm^3 and$14 \times 14 \times 0.15$ cm^3, respectively, making 1.9-cm thick FSC. The nominal foldcore density (calculated as the mass of the foldcore divided by the volume between two face-sheets) was 250 (kg/m^3). Note that aluminum and aramid fiber honeycomb cores have densities ranging from 10-140 (kg/m^3) depending primarily on thickness [15] and foam cores have densities ranging from 50-200 (kg/m^3), also depending on thickness [16]. The current study presents initial efforts to develop foldcore for HVI applications, and the eight-ply CFRP foldcore and face-sheets were prepared as reference. The foldcore density can be easily controlled by adjusting unit-cell dimensions (Fig. 3) and using less plies and lighter materials. If foldcores are proven to have a great advantage over honeycomb and foam cores in HVI performance, its higher density may be acceptable (depending on the requirements of the applications).

HVI TESTING

HVI testing was done in collaboration with the Texas A&M University HVI Laboratory [17]. A two-stage light gas gun (2SLGG) capable of accelerating 2–10 mm diameter projectiles of varying shapes (spherical, ogive, cylindrical, buckshot, *etc.*) to 2–8 km/s was used to perform HVI experiments. Ultra-high-speed shadowgraphy imaging (10M fps) with a Shimadzu HPV X-2 camera was used to

characterize the HVI experiments. Detailed operational capabilities and the methodology of the 2SLGG can be found in [17, 18]. All FSC target specimens (nominal thickness t = 18 mm) were impacted with aluminum 2017 spheres (nominal diameter D = 4 mm, mass 0.094 g).

The FSC targets were sandwiched between two 30.5 × 30.5 × 0.1 cm3 A-36 steel plates (Fig. 5a), each having a 10.2 cm diameter circular cutout (aperture) in the center. The target assembly, consisting of the two steel plates and the target specimen, was held together by fasteners that surround the cutout, effectively inducing clamped axisymmetric boundary conditions on targets. The target assembly was fixed rigidly in a target fixture that was mounted at either normal or oblique angles to the interior of the 2SLGG target tank. The target assembly was aligned within the target tank such that the axis of projectile flight was aligned with the center of the target specimen as shown in Fig. 5b. The high-speed camera was positioned outside the 2SLGG target tank viewing the target through the optical access window. The axis of camera viewing is oriented orthogonal to the projectile path and parallel to the plane of the target specimen (Fig. 5b).

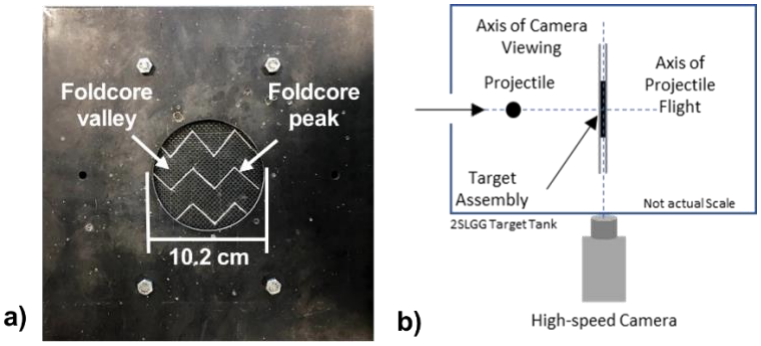

Figure 5. a) An FSC target sandwiched between two A-36 steel plates with a circular aperture. b) Schematic of the positioning of the target and the camera relative to the axis of projectile flight.

RESULTS AND DISCUSSION

A total of four HVI tests were conducted on FSCs. As stated previously, the foldcore and face-sheets were each fabricated by curing eight plies of AS4/3501 woven fabric prepregs stacked in a $[0]_8$ sequence. Each FSC target was mounted by a combination of two impact angles, normal (0°) and oblique (45°), and two open channel directions (vertical and horizontal, Fig 6).

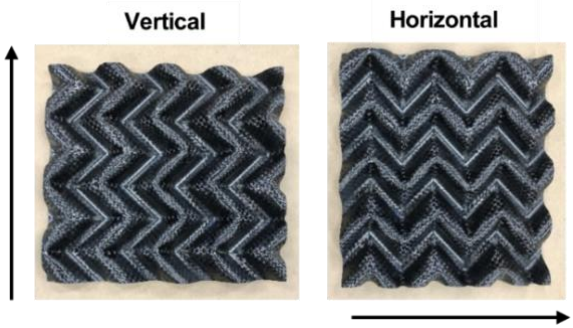

Figure 6. Foldcore channel orientation.

TABLE II includes the HVI test parameters – impact angle, channel orientation, impact velocity (V_{imp}), and impact location (peak or valley, cf. Fig. 3); results – target of mass loss (%) and representative hole geometry on the target impact face. Each FSC target was impacted by a 4-mm diameter Al 2017 sphere at a nominal velocity of 3 km/s (ranging from 2.7-3.3 km/s). The FSC's open channel direction is also important when capturing the anisotropic fragments cloud expansion after HVI event. Fig. 7 gives the front and back faces images after the HVI tests. The entry holes are nearly circular in normal impacts and elliptical in oblique impacts. The oblique entry and exit holes are displaced vertically while the normal entry and exit holes are level (Fig. 7). The FSC-0-H target exhibited two exit holes due to the projectile and guided FSC fragments. More details are discussed in the following.

TABLE II. HVI EXPERIMENTAL DATA OF THE CFRP FSC TARGETS

Test ID	Impact Angle (°)	Channel Orientation	V_{imp} (km/s)	Impact Location	Impact Damage Shape	Exit Damage Shape	Target Mass Loss (%)
FSC-0-H	0	Horizontal	3.305	Foldcore Peak	Circle	Two Irregular Holes	0.59
FSC-0-V	0	Vertical	3.149	Foldcore Valley	Circle	Circle	0.23
FSC-45-H	45	Horizontal	3.000	Foldcore Valley	Ellipse	Irregular	0.30
FSC-45-V	45	Vertical	2.744	Foldcore Valley	Ellipse	Ellipse	0.19

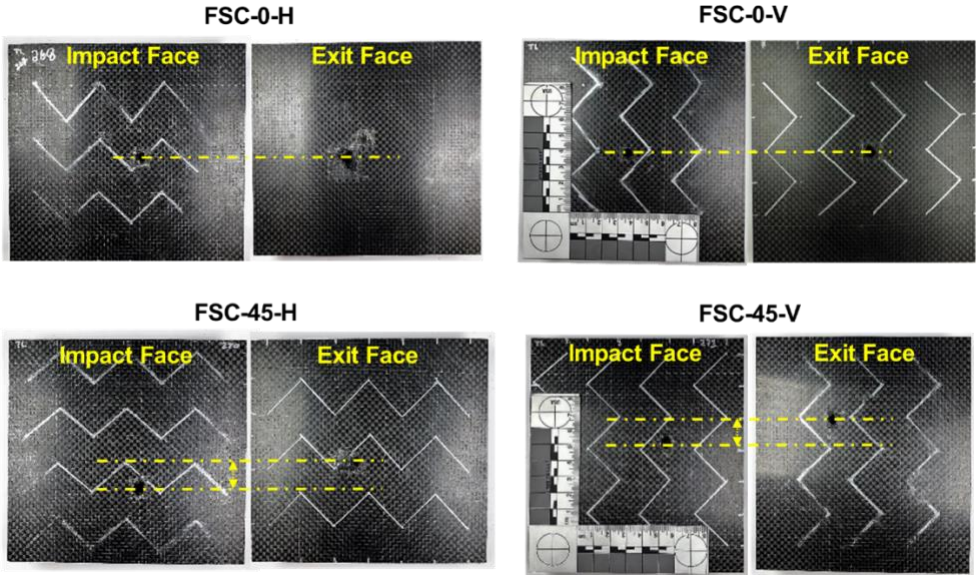

Figure 7. FSC impact and exit face damage

A series of the shadowgraph images taken for FSC targets subjected to normal and oblique impacts, two zoomed-in images of incoming projectile and the debris (or fragmentation) cloud expansion at 12.8 μs, and the exit hole are used to characterize the HVI events. Two normal (0° impact angle) HVI experiments performed on the FSC target with horizontal and vertical open channel directions are shown in Fig. 8.

As can be seen in these images, the back-face debris cloud velocity was not co-linear with that of the incoming projectile; a fraction of fragmentation was redirected due to confined foldcore architecture in normal impact; two exit penetration holes were observed in FSC under the normal impact (Fig. 8a), caused by redirected fractured projectile fragment. Neither of these exit holes are in line with the projectile's entry path, indicating the projectile was deflected and possibly split apart as it impacted the foldcore peak. The off-center double exit holes were not observed in the FSC-0-H target (Fig. 8b). Note that the redirection of the incoming projectile or FSC fragmentation depends on an impact location (*i.e.* peak or valley of foldcore, cf. Fig. 3). An impact location may be misaligned when mounting the FSC targets, thus it can be random factor. Two exit penetration holes were observed only in the FSC-0-H target (Fig. 8). Therefore, additional tests are required to fully understand the effects of a projectile impact location on the FSC HVI response. There was noticeable difference in debris cloud formation and expansion during an HVI event between two FSC targets (FSC-0-H and FSC-0-V) subjected to normal impact. The debris clouds formed a convergent shape in the FSC-0-H target, but was divergent in the FSC-0-V. The only differences between these FSC targets are the open channel orientation and impact location. Assuming that one controlling factor in debris cloud shape/expansion is open channel orientation, the foldcore orientation causes the ejecta to fan out in the direction of the foldcore channel. The FSC-0-H is viewed down the length of the channels, so this fanning out is not in the plane of view. Additional normal impact tests will confirm this phenomenon in the future.

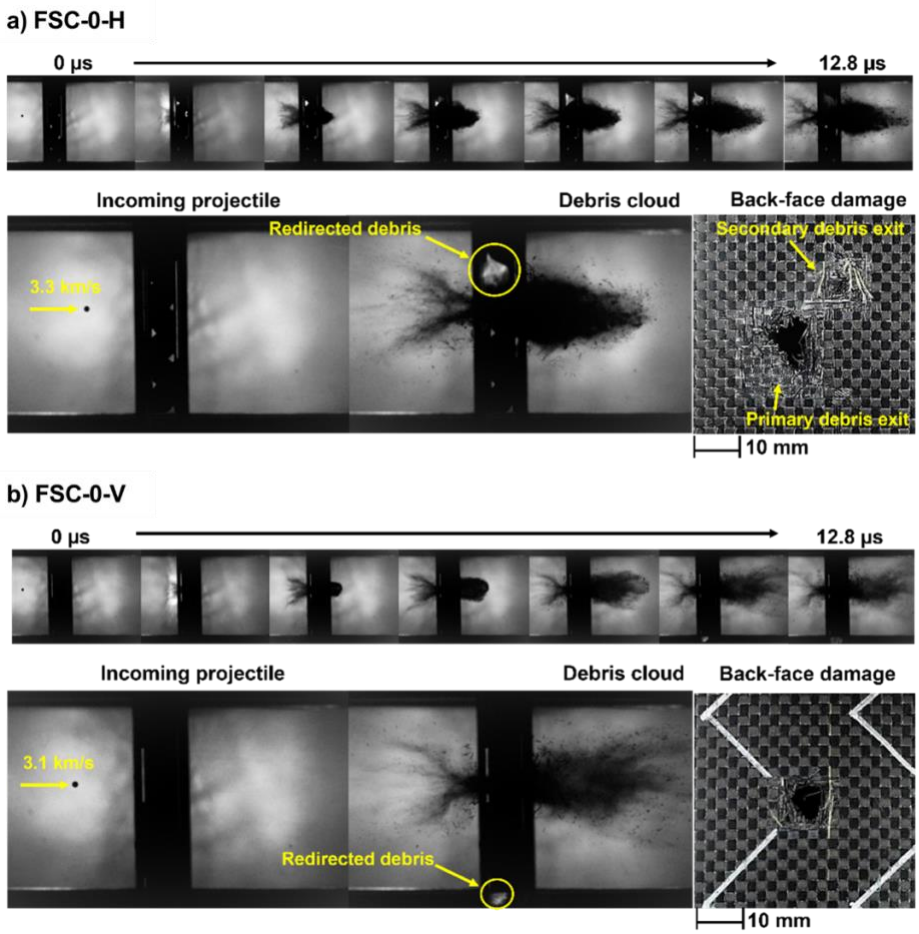

Figure 8. HVI testing on the FSC targets subjected to normal (0°) impact.

Fig. 9 shows a summary of HVI tests performed on the FSC target subjected to oblique impact. Similar to the normal impact (Fig. 8), the debris cloud formed and expanded throughout the core's open channels in the FSC targets. The back-face debris cloud was much smaller than that from normal HVI tests. In Fig. 9, the lines drawn on the back of the FSC targets show the approximate locations of foldcore peaks. This indicates that the projectile exited near the foldcore peak in the FSC-45-H target and at the area between two foldcore peaks. Comparing hole geometries and damage morphologies, the HVI response of FSC targets is highly influenced by the impact location and angle of incoming projectile. In general, more back face damage was observed when the foldcore was oriented in the horizontal direction (both for FSC-0-H and FSC-45-H targets; cf. back-face damage in Figs. 8 and 9).

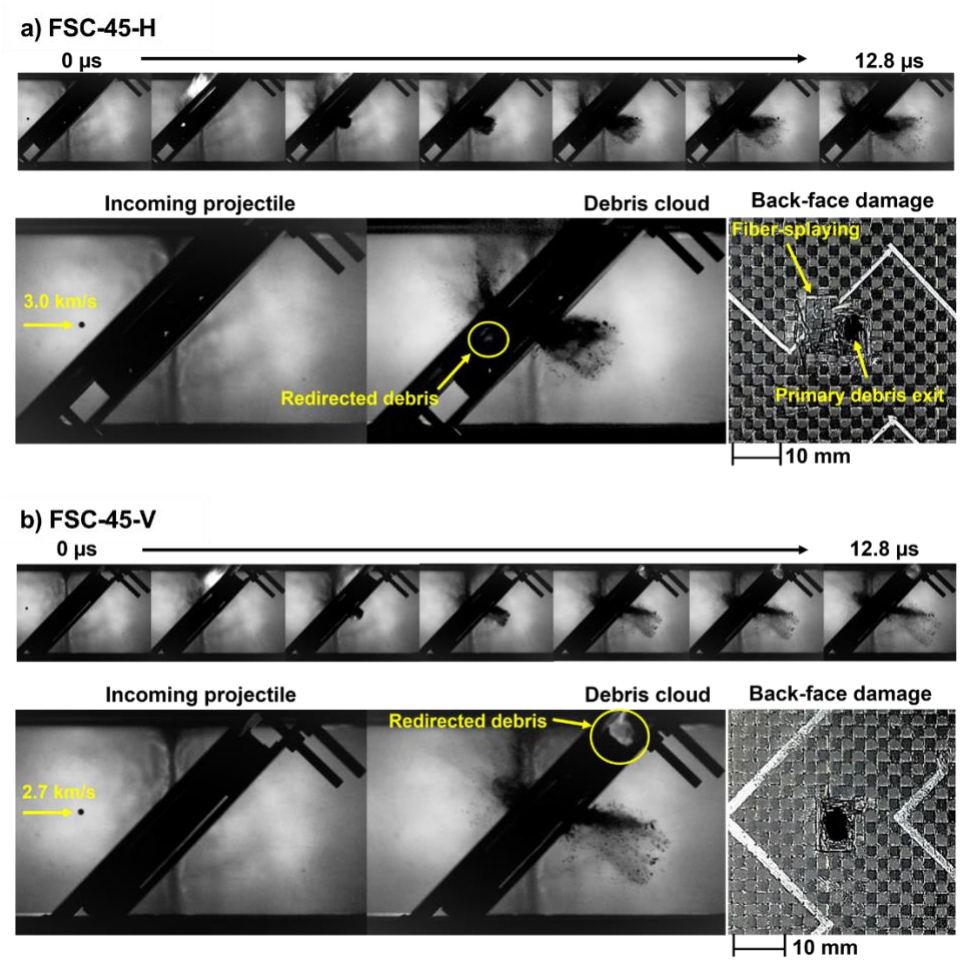

Figure 9. HVI testing on the FSC targets subjected to oblique (45°) impact.

An important characterization of HVI performance in this study is exit-damage area (Figs. 10 and 11). The quantitative assessment of HVI damage in FSC targets were performed by approximating the area of the exit penetration hole and surrounding fractured and delaminated face-sheet. The FSC-0-H had the largest exit damage area of 550 mm^2. The other three FSCs had more localized damage. As local damage is a typical of CFRP HVI events, a larger exit damage area indicates the projectile fragments were broken and dispersed more by the foldcore or had a lower

velocity. Either case (dispersed or slowed fragments) lowers the impact energy per unit area as the velocity or mass of the impacting particle is reduced. The FSC-0-H and FSC-45-H targets both exhibit significant areas of fiber-fracture and fiber-splaying (laminate that flexed outward but did not completely fracture). This indicates projectile and debris with lower kinetic energy. The greater mass loss, exit-damage area, and fiber-splaying can be attributed to the projectile impacting a foldcore peak of FSC-0-H, indicating dependence of FSC performance on impact location.

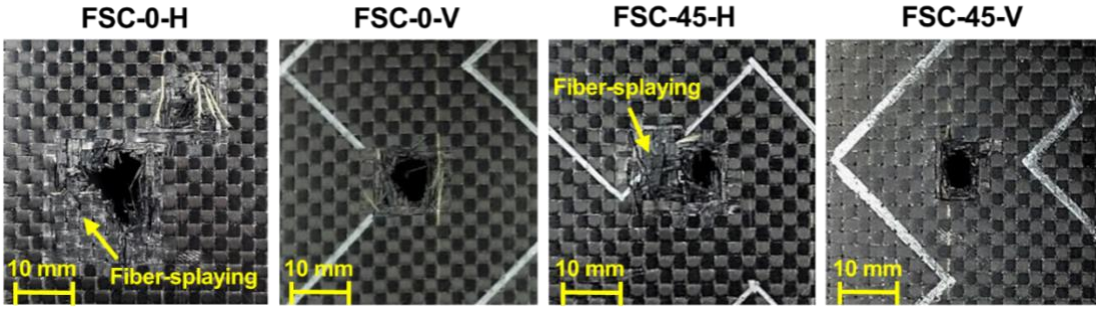

Figure 10. Exit face damage in FSC targets.

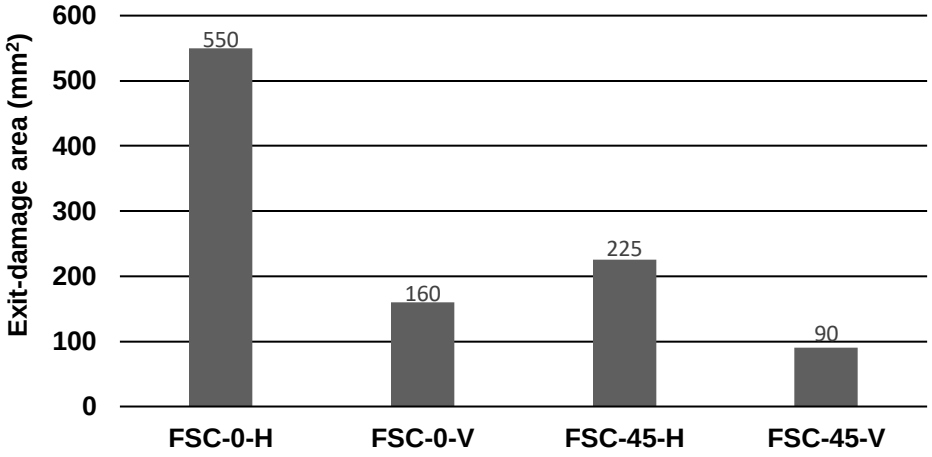

Figure 11. Bar graph of Exit-damage area values.

The HVI tests results suggest preferentially oriented face-sheets and foldcore materials can successfully redirect the fragmentation debris and, perhaps, maximize HVI energy absorption. In this work, we performed the qualitative/quantitative assessment of HVI-induced damage in FSC targets and debris cloud formation/expansion. Further HVI tests with various projectile velocities will be beneficial for developing a ballistic limit curve, known as performance metric for HVI shield tests [19].

CONLCUSION AND FUTURE WORK

This paper presents the hypervelocity impact (HVI) test results for foldcore sandwich composites (FSCs) subjected normal (0°) and oblique (45°) impact with a nominal velocity of 3 km/s. The foldcore and each face-sheet were prepared with eight layers of carbon/epoxy woven fabric prepregs. The following key conclusions are drawn:

- The foldcores successfully redirected HVI projectiles and manipulated debris cloud formation/expansion. The debris cloud propagated through the foldcore open channels in a directional orthogonal to the projectile path. The back-face debris clouds fanned out in foldcore channel direction.
- The HVI response of FSC targets strongly depends on the impact location and angle of incoming projectile. This suggests that FSCs prepared with optimal core architecture and materials may perform better than conventional sandwich panels during an HVI event.

This work presents initial efforts to design FSCs for protective structures under HVI loading. Additional studies are required to fully understand the high strain-rate response of FSC targets. More detailed inspection of FSCs after HVI testing through non-destructive evaluations and destructive sectioning will be performed to better characterize the effects of foldcore (unit-cell) geometry, size, and material selection on HVI mitigation.

ACKNOWLEDGMENTS

This research would not have been possible without the support of the USU Engineering Undergraduate Research Program fellowship. Thanks also to the USU Metal Factory and USU Engineering Machinist Terry Zollinger for his assistance in mold manufacturing. The authors would like to acknowledge Mr. Paul Mead, Mr. Jacob Rogers, and team of the TAMU Materials for Extreme Environments group for their support in operating the two-stage light gas gun for the Hypervelocity Impact testing.

REFERENCES

1. Heimbs, S. 2012. “Foldcore sandwich structures and their impact behaviour: An overview.” *Dynamic Failure of Composite and Sandwich Structures*, 491–544.
2. Gattas, J. M. & You, Z. 2015. “The behaviour of curved-crease foldcores under low-velocity impact loads.” *International Journal of Solids and Structures*, 53, 80–91.
3. Gattas, J. M. and You, Z. 2014. “Quasi-static impact of Indented foldcores.” *International Journal of Impact Engineering*, 73, 15–29.
4. Fathers, R. K., Gattas, J. M., and You, Z. 2015. “Quasi-static crushing of eggbox, Cube, and modified Cube foldcore sandwich structures.” *International Journal of Mechanical Sciences*, 101-102, 421–428.
5. Du, Y., Song, C., Xiong, J., and Wu, L. 2019. “Fabrication and mechanical behaviors of carbon fiber reinforced composite foldcore based on curved-crease origami.” *Composites Science and Technology*, 174, 94–105.
6. Liu, B., Sun, Y., Sun, Y., and Zhu, Y. 2019. “Fabrication and compressive behavior of carbon-fiber-reinforced cylindrical foldcore sandwich structure.” *Composites Part A: Applied Science and Manufacturing*, 118, 9–19.

7. Elsayed, E. A., and Basily, B. 2004. “A continuous folding process for sheet materials.” *International Journal of Materials and Product Technology*, 21, 217.
8. Miura, K. 1972. “Zeta-Core Sandwich-Its Concept and Realization.” *Institute of Space and Aeronautical Science, University of Tokyo, Report No. 480*, 137–164.
9. Rastogi, M. 2016. “Moisture ingress in honeycomb sandwich composite structures – effects detection.” *International Journal of Engineering Research and Technology*, V5, 171–176.
10. Ryan S. and Christiansen E. 2015. “Hypervelocity impact performance of open cell foam core sandwich panel structures.” *Tech. Rep., NASA TM-2015-218593. NASA Johnson Space Center, Houston: NASA.*
11. Heimbs S., Cichosz J., Klaus M., Kilchert S., and Johnson A. F., 2010. “Sandwich structures with textile-reinforced composite foldcores under impact loads,” *Composite Structures*, 92, 6, 1485–1497.
12. Heimbs, S., Middendorf, P., Kilchert, S., Johnson, A.F. and Maier, M., 2007, September. “Numerical simulation of advanced folded core materials for structural sandwich applications” *1st CEAS European Air and Space Conference*, 2889-2895.
13. HexForce. 3k Carbon Fiber AGP193-P, *Hexcel Datasheet*.
14. HexPly. Epoxy 3501-6, *Hexcel Datasheet.*
15. PAMG-XR1 5056 aluminum honeycomb core. *Plascore*.
16. PET foam, *CEL COMPONENTS Datasheet.*
17. The Texas A&M University Hypervelocity Impact Laboratory, Retrieved June 14, 2022, from telacyjr.engr.tamu.edu/facility/hypervelocity-impact-laboratory-hvil/.
18. J. A. Rogers, A. Mote, P. T. Mead, K. Harrison, G. Lukasik, K.R. Kota, W.D. Kulatilaka, J. Wilkerson, and T.E. Lacy Jr. 2022. “Hypervelocity impact response of monolithic UHMWPE and HDPE plates,” *International Journal of Impact Engineering*, 161, 104081.
19. Schonberg, W. P., 2016. “Concise history of ballistic limit equations for multi-wall spacecraft shielding.” *REACH*, 1, 46–54.